SCISPACE
formerly Typeset

Open access • Book Chapter • DOI:10.1007/978-1-4684-1048-8_9

Xenon Shock Waves Driven by High Magnetic Fields — Source link

J. W. Shearer, J. W. Beasley, A. Reyenga, D. Steinberg

Institutions: Lawrence Livermore National Laboratory

Published on: 01 Jan 1980

Topics: Shock tube, Shock wave, Xenon, Shock (fluid dynamics) and Magnetic field

Related papers:

- Microwave Investigation of Electrically Driven Shock Waves in Gases
- Enhancement of ionization behind strong shock waves in argon near the shock tube walls
- The relaxation phenomena in an ionized shock front
- Wall shocks in high-energy-density shock tube experiments
- Investigation of shock compressed plasma parameters by interaction with magnetic field

Share this paper:

View more about this paper here: https://typeset.io/papers/xenon-shock-waves-driven-by-high-magnetic-fields-2lasknspce

CONF-790540--40

MASTER

PREPRINT UCRL- 82194

Lawrence Livermore Laboratory

XENON SHOCK WAVES DRIVEN BY HIGH MAGNETIC FIELDS

J. W. SHEARER, J. W. BEASLEY, A. REYENGA, AND D. STEINBERG

May, 1979

PREPARED FOR SUBMISSION TO THE 2ND INTERNATIONAL CONFERENCE
ON MEGAGAUSS MAGNETIC FIELD GENERATION AND RELATED TOPICS
MAY 29 - JUNE 1, 1979, WASHINGTON, DC

This is a preprint of a paper intended for publication in a journal or proceedings. Since changes may be made before publication, this preprint is made available with the understanding that it will not be cited or reproduced without the permission of the author.

XENON SHOCK WAVES DRIVEN BY HIGH MAGNETIC FIELDS

James W. Shearer, James W. Beasley, Arnold Reyenga, and Daniel Steinberg

Lawrence Livermore Laboratory
Livermore, CA 94550

Magnetic fields in the range 0.2 - 2.0 MG produce shocks in 0.1 - 1.0 atmosphere xenon gas which have shock mach numbers as high as 100. Using pulsed x-ray and other diagnostics, our studies of velocity, compression, and luminosity are in good agreement with a simple snowplow theory. In some of the experiments, ultraviolet radiation from the shocked xenon produces luminous precursors and interactions with the metal walls of the shock tube. The addition of an ultraviolet absorbing organic impurity vapor diminishes the amplitude of these effects. A clean, chemically inert metal wall is even more effective. Further experiments show that magnetic shear has a stabilizing effect on the current-carrying layer of the shocked gas. We conclude that a megagauss magnetic field is a useful shock tube driver for producing high velocity shock waves.

"Work performed under the auspices of the U.S. Department of Energy by the Lawrence Livermore Laboratory under contract number W-7405-ENG-48."

NOTICE

This report was prepared as an account of work sponsored by the United States Government. Neither the United States nor the United States Department of Energy, nor any of their employees, nor any of their contractors, subcontractors, or their employees, makes any warranty, express or implied, or assumes any legal liability or responsibility for the accuracy, completeness or usefulness of any information, apparatus, product or process disclosed, or represents that its use would not infringe privately owned rights.

NOTICE

"This report was prepared as an account of work sponsored by the United States Government. Neither the United States nor the United States Department of Energy, nor any of their employees, nor any of their contractors, subcontractors, or their employees, makes any warranty, express or implied, or assumes any legal liability or responsibility for the accuracy, completeness or usefulness of any information, apparatus, product or process disclosed, or represents that its use would not infringe privately-owned rights."

December 1, 1978

Xenon Shock Waves Driven by High Magnetic Fields

James W. Shearer, James W. Beasley*,
Arnold Reyenga, and Daniel Steinberg

Lawrence Livermore Laboratory

1. Introduction

This paper describes some experiments on the application of megagauss magnetic field techniques[1,2,3] to produce strong shock waves[4,5] in xenon gas. The magnetic fields are produced by capacitor banks and high explosive generators that are described elsewhere.[6,7]

Consider the one-dimensional snowplow model of a gas or plasma sheath driven by a magnetic field (Fig. 1). From Newton's second law:

$$\frac{B^2}{2\mu_0} = \sigma \frac{du}{dt} + u V \rho_0 \tag{1}$$

where B is the magnetic field, μ_0 is the vacuum magnetic permeability, u is the velocity of the shocked gas, ρ_0 is the initial unshocked density, V is the shock velocity, and σ is the mass per unit area of the snowplowed sheath:

$$\sigma \equiv \int_{x_0}^{x} \rho_0 \, dx \tag{2}$$

where x is the position of the sheath. For simplicity we neglect compressional and radiation effects inside the sheath, and we also assume that the sheath is a good enough conductor to prevent appreciable diffusion of the magnetic field towards the shock discontinuity.

Consider a strong shock for which

* Present Address: 8th Naval District, New Orleans, LA 70146

$$V/u = (\gamma + 1)/2 \tag{3}$$

where γ is the specific heat ratio. Consider also a steady state where B and u are constants; then from equs. (1) and (3):

$$V = \left(\frac{\gamma + 1}{4 \mu_0 \rho_0}\right)^{1/2} B \tag{4}$$

This result is displayed in Fig. 1 for the Case $\gamma = 1.4$. Conventional shock tubes are designed to be reusuable; thus their driving pressures are less than a few hundred atmospheres, corresponding to $B \lesssim 0.1$ MG. On the other hand, high explosive systems have characteristic expansion velocities which are less than 1.0 cm/μsec. Thus, for $\rho \geq 400$ atm and $V \geq 1.0$ cm/μsec, megagauss field shock pistons are quite competitive. The alternatives are elaborate convergent high explosive systems, rockets, or nuclear explosives[8] all of which have many obvious disadvantages.

In our experiments eqn (4) can be checked because ρ_0, B, and V are all measured quantities, and γ can be found from the strong shock equation:

$$\gamma = (\eta + 1)/(\eta - 1) \tag{5}$$

where η is the density compression ratio ρ/ρ_0 of the shocked gas. Temperature measurements are not available, but useful inferences about the shocked xenon can be drawn from strong shock theory. The equality of the kinetic energy density with the internal energy density in a strong shock can be written:

$$\frac{1}{2} n_x M_x U^2 = \frac{3}{2} k (n_x T_x + n_e T_e) + \overline{I}_Z \tag{6}$$

where n_x is the xenon density (atoms plus ions), n_e is the electron density, M_x is the mass of a xenon atom (or ion), and $\overline{I}_Z$ is the ionization energy per

xenon atom. T_x and T_e are the respective ion and electron temperatures. Were one to assume that the shocked xenon is not ionized, then $n_e = 0$ and $I_z = 0$, and from eqn (6) one would estimate $T_x \gtrsim 1$ keV for $B \gtrsim 1$ MG, $\gamma = 1.4$ and $\rho_0 \simeq 5.6 \times 10^{-3}$ gm/cm^3, (atmospheric density). This obviously unrealistic result implies that the xenon is actually ionized to a plasma state at some lower temperature.

Further discussion of the equation of state of the shocked xenon is beyond the scope of this paper. Our more modest aim is to demonstrate that the megagauss shock tube is a useful experimental method for studying strong shocks, corresponding to shock Mach numbers of 100 or more.

2. Magnetically-Driven Shock-Wave Box

A rectangular shock wave box is used, as shown in Fig. 2. The metal plate conductors are 100 mm wide and 100 mm long; they are separated by a 10 mm gap. Various metallic surfaces are used, as described later in this paper. The breech end of the box is attached to the capacitor bank plates with heavy flanges. A lucite insulator separates the flanges, and it is plated on the shock tube face with a 50 nm coating of aluminum. This metal coating provides an initially uniform conduction path for the current, and it blows up into a conducting plasma on a submicrosecond time scale, thus preventing localized arc formation. The other two sides and the muzzle end of the shock wave box are constructed of transparent plastic, which provides mechanical rigidity, makes the box gas tight, permits optical diagnostics, and is transparent to x-rays.

The breech end of this shock wave box is connected to the transmission line from a fast capacitor bank by techniques similar to those used in the single turn megagauss coil experiment.[7] However, the maximum magnetic field is lower in these experiments because the width of the current sheet is 10 cm rather than 1 cm. However, even at this field level the plastic is shattered and the metal surfaces are damaged, so a fresh box must be assembled for each experiment. Protection from flying shrapnel and noise is provided by a thick-walled room.

Conventional magnetic probes are located in the connection plate to measure the capacitor discharge current; in a few experiments additional probes are inserted into the gas volume through an insulated hole in the metal wall. A rotating mirror framing camera observes the self-luminous gas sheath from the side and from the end. The most useful diagnostic tool, however, is the pulsed

x-ray radiography,[9] which observes the xenon gas density distribution in the shock tube. The pulsed x-ray source is a 50 ns (FWHM) 85 kV (peak) field emission tube designed and fabricated at the Lawrence Livermore Laboratory.[10] The x-ray source has a diameter of about 2 mm, and is located about 2 m away from the shock tube. The x-ray film is mounted close to the shock tube behind a protective cover of aluminum; the image is well resolved, and only about 6% larger than the experiment.

A possible source of error is the perturbing effect of the return flux of magnetic field, some of which appears as a reverse magnetic field ahead of the shock. However, probe signals show that this reverse field is less than one third of the main magnetic field. This corresponds to a pressure of less than 10% of the driving pressure, and does not seriously modify the main effects observed. Another possible source of error is the effect of the field concentration along the sides of the box next to the plastic side wall; one might expect to see magnetic pinching at that point, for example. However, the clarity of the x-ray radiography pictures (as shown later in this paper) is strong evidence that such effects are not important. Two other sources of error are the interaction of the shock wave with the metal walls, and the Rayleigh-Taylor instability at the current sheath. These will be described below.

A typical set of pulsed x-ray pictures from this shock tube box is displayed in Fig. 3. Each of these pictures is taken from a separate experiment, but the optical and electrical measurements indicate that there is good reproducibility from shot to shot. In addition, the optical measurements show that the light front coincides with the shock front density jump for this series of experiments. Further aspects of these pictures are discussed in subsequent sections.

3. Shock Velocity vs Time

Results for one atmosphere xenon shock experiments are plotted in Fig. 4; the data are similar to the half-atmosphere xenon results shown in Fig. 3. At late times both the magnetic field and the shock velocity approach the steady state approximation of eqn (4) and Fig. 1.

Table I compares these steady state measurements with the simple snowplow theory, and it also tabulates a few other measurements made on faster capacitor banks. We find general agreement between experiment and theory over a density range of 8 and a magnetic pressure range of 7.

As noted in the table, measurements of shock velocity V are more difficult for V > 2 cm/μsec. In this range the light front is seen to be ahead of the density jump. This "optical precursor" is consistent with other strong shock studies,[11] which suggest that it is caused by strong radiative effects. For these cases velocity values in Table I are taken from the optical records because there were not enough experiments done to accumulate a useful sequence of x-ray pictures. Despite the loss in accuracy from this procedure, there is still good agreement between calculated and experimental shock velocities.

Table I

Peak Shock Velocities - Theory vs. Experiment

Xenon Fill		Peak Field	Peak Velocity V/cm/μsec)	
P (atm)	ρ_0 gm/cm^3	B (MG)	Measured	Calculated[a]
1	.0056	.35[b]	1.2	1.02
1/2	.0028	.35[b]	1.5	1.45
1/8	.0007	.4[c]	$\simeq$ 3[d]	3.3
1/2	.0028	.9[c]	$\simeq$ 4[d]	3.7

(a) Calculations assume $\gamma = 1.4$ in eqn (4)

(b) The inductance of the capacitor bank is much greater than that of the shock tube; therefore, to first approximation the magnetic field is not perturbed by the change in xenon fill density.

(c) For these experiments, lower inductance capacitor banks were employed.

(d) Approximate estimates based on optical records; see text.

4. Interaction of Shock with Metal Walls

In addition to the optical precursors mentioned above, we observe "wall precursors" in many of our experiments. These are the wedge-shaped shock formations which are seen next to the iron rails ahead of the main shock in Fig. 3. Our experiments show that the size of these wall precursors can be changed by adding an organic vapor impurity to the xenon or by changing the metal surface of the rails. We believe that both experiments support the idea that the optical precursor is a radiative effect, similar to the precursor seen elsewhere in explosive-driven argon shock tubes.[12]

We add the organic vapor propene (propylene, C_3H_6) to the xenon gas. This contaminant absorbs ultraviolet radiation in the 100-200 nm wavelength range; xenon, however, is transparent in this range. The x-ray pictures in Fig. 5 show that the wall precursor is substantially reduced by this contaminant.

Various metals were tested as rail surfaces; iron, lead, and aluminum rails all support wall precursors. On the other hand, clean surfaces of gold, rhodium, and iridium (all plated on aluminum) do not support wall precursors. Figure 6 demonstrates this result for iridium (compare with Fig. 3). The importance of surface cleanliness is also demonstrated; the presence of machinist's oil causes the wall precursor to reappear.

It appears that the rail surface which absorbs the high radiation flux from the xenon shock is crucial. If it is nonmetallic, such as an oxide or an oil layer, it is rapidly heated by the radiation and explodes, thereby producing a secondary shock ahead of the principal one. On the other hand, if the rail surface is truly metallic, thermal conduction keeps it cool enough to remain passive. Our shock tubes are assembled in the open air of

the laboratory; apparently only gold, rhodium, and iridium are chemically inert enough to resist surface oxidation under such conditions.

We conclude that inert metal surfaces (and possibly organic contaminants) are useful techniques to keep the shock one-dimensional by suppressing wall precursors.

5. Stabilization of Current Sheath Surface by Magnetic Shear

Although the leading edge of sheaths moving between iridium-plated-walls was quite flat, the rear current-carrying surface of the snowplowed xenon sheath showed a Rayleigh-Taylor instability of rather large amplitude (Fig. 6a-6c). Consequently, it was suggested that we try to stabilize this effect by means of magnetic shear.[13]

An experimental setup (Fig. 6d) was designed which provided 10 kilogauss of transverse field across the breech of the xenon shock box. The best results were obtained when the thin aluminum film was located in the center of the magnet gap. The amount of this transverse flux which was trapped in the xenon sheath, and its subsequent history, were not directly measured. We do know that the transverse field had a favorable effect (see Fig. 6e-6f), almost completely damping out the instability.

Our explanation for this result is that some of the transverse flux is trapped in the xenon plasma sheath when the current sheath is first formed, and is then carried along with the xenon sheath as it moves. Precise estimates of the magnitude and direction of this flux are difficult. Resistive diffusion diminishes the field; compression of the xenon in the sheath increases it. "Stretching" of the field lines as the sheath moves away from the pole pieces should increase the magnetic energy and lead to magnetic field line reconnection behind the sheath.

Whatever the details, the experiment demonstrates improved one-dimensionality of the current-carrying layer of the xenon sheath (Fig. 6). Thus, the results support the suggestion that magnetic shear tends to stablize the Rayleigh-Taylor instability.

6. Explosive-Generator-Driven Xenon Shocks

Our shock wave box can also be driven by a high explosive generator[6] instead of a capacitor bank. However, if the generator were connected directly to the box, the slowly rising ($\simeq 50\,\mu$sec) early current profile would gently sweep the xenon out before the main high current pulse is generated. Consequently, it is necessary to switch the generator current into the shock tube box just before the final energy burst is created.

We use the magnetohydrodynamic switch which is described in a companion paper.[14] Briefly, it is a short "exploding foil" liner which is deliberately shaped to be unstable after it explodes, so that the magnetic forces push most of its mass aside, leaving a comparatively small mass of current-carrying plasma in the shock-wave box. The generator design is the "flat plate" geometry described elsewhere.[6]

The pulsed x-ray radiographs do not show a sharply defined shock front in these experiments; probably it is not straight because of uneven blowup of the magnetohydrodynamic switch. High speed camera measurements reveal an optical precursor moving at 4.0 $\pm$ 0.5 cm/ sec in the 1/2-atmosphere xenon fill, similar to the highest speed experiment in Table I. Assuming that the sheath moves at the same speed as the optical precursor, one infers that a magnetic field of approximately one megagauss is present.

One radiometry experiment was done using a filter-photoelectric detector combination centered at 547.5 nm with a bandwidth of 45.0 nm (at 1% of peak). Two of these combinations were aimed at normal incidence (0°), two were at 60°, and all four subtended a solid angle of 4.3×10^{-5} sterradians. They were calibrated from a glowing tungsten source of known brightness, and all of them measured a shock wave brightness corresponding to temperatures

in the 2-4 eV range. This result agrees with similar brightness measurements in xenon in this density and velocity range.[15]

7. Summary

Our results indicate that megagauss magnetic fields can be used as a shock tube driver for velocities greater than 1 cm/μsec at near-atmospheric densities. The work was done several years ago using power supplies available at that time.[6,7] Today, at the time of this Megagauss II conference, more powerful capacitor banks and faster pulsed-power systems are in existence. Thus, the potential range of shock Mach numbers (at atmospheric density) can be extended to even higher values, perhaps approaching M = 1000 for xenon. Many interesting physical effects can be anticipated by those who undertake such studies.

8. Acknowledgements

The late E. J. Faria assisted all of the experimental work; W. M. Trimble performed the radiometry experiment. The authors benefited from discussions with F. Abraham, C. Aplin, R. Duff, J. LeBlanc, C. McDonald, and J. Wilson.

Reference to a company or product name does not imply approval or recommendation of the product by the University of California or the U.S. Department of Energy to the exclusion of others that may be suitable.

References

1. Proceedings of "Conference on Megagauss Magnetic Field Generation by Explosives and Related Experiments," (Frascati, Sept. 1965) Ed by H. Knoepfel and F. Herlach, EURATOM Report EUR 2750.e, Brussels, July, 1966.

2. F. Herlach, "Megagauss Magnetic Fields," pp. 341-417 of Reports on Progress in Physics, 25 (1968).

3. Heinz Knoepfel, "Pulsed High Magnetic Fields" North Holland Publishing Co., Amsterdam (1970).

4. Ya. B. Zel'dovich and Yu. P. Raiser, "Physics of Shock Waves and High Temperature Hydrodynamic Phenomena," ed. by Wallace D. Hayes and Ronald F. Probstein, Academic Press, New York, (Vol. 1, 1966. Vol II, 1967).

5. John W. Bond, Jr., Kenneth M. Watson, and Jaspar A. Welch, Jr., "Atomic Theory of Gas Dynamics," Addison-Wesley Publishing Company, Reading, Massachusetts, (1965).

6. J. W. Shearer, F. F. Abraham, C. M. Aplin, B. P. Benham, J. E. Faulkner, F. C. Ford, M. M. Hill, C. A. McDonald, W. H. Stephens, D. J. Steinberg, and J. R. Wilson, "Explosive-Driven Magnetic-Field Compression Generators," J. of Appl. Phys, 39, No. 4, pp. 2102-2116 (March, 1968).

7. J. W. Shearer, "Interaction of Capacitor-Bank-Produced Megagauss Magnetic Field with Small Single-Turn Coil," J. of Appl. Phys., 40, No. 11, pp. 4490-4497 (October, 1969).

8. "The Effects of Atomic Weapons," (1st edition) ed. by Samuel Glasstone, et al, McGraw-Hill, New York (1950) - quoted extensively in ref. 4.

9. J. P. Dyke, Scientific American, 210, No. 1, pp. 108-118 (Jan. 1964).

10. Kerry L. Bahl and Harry C. Vantine, "A Flash Radiographic Technique Applied to Fuel Injector Sprays," Proceedings of the Flash Radiography Symposium, Houston, Texas, September 28, 1976, (Available from American Society for Nondestructive Testing,, 3200 Riverside Drive, Columbus, Ohio, 43221, or from LLL (UCRL 78280, Preprint)).

11. Reference 4, Chapter VII.

12. R. G. Shreffler and R. H. Christian, "Boundary Disturbances in High Explosive Shock Tubes," J. Appl. Phys., 25, 324-331 (1954).

13. Stephen E. Bodner, private communication.

14. Daniel J. Steinberg, et al, LLL Report in preparation.

15. A. E. Voitenko, I. Sh. Model', and I. S. Samodelov, "The Brightness Temperature of Shock Waves in Xenon and Air," Doklady Akademii Nauk, SSR, 169, pp. 547-549 (1966) [English Translation Sov. Phys. Doklady 11, pp. 596-598 (1967)].

FIGURE CAPTIONS

Figure 1: Snowplow model of shock velocity V versus magnetic field B for various initial densities ρ_0 at $\gamma = 1.4$.

Figure 2: Sketch of rectangular magnetically-driven shock wave box with top cover removed and top of mylar sheets cut back.

Figure 3: Sequence of positive prints of pulsed x-ray radiographs of xenon snowplow for half-atmosphere xenon fill driven by $\sim$ .3 MG magnetic field. Note the sharp boundaries of the dense xenon, the greater transparency of the low density region of the magnetic piston, and the wedge-shaped wall precursors along the iron rails.

Figure 4: Shock position x and magnetic field B vs time for atmospheric xenon.

Figure 5: Positive prints of pulsed x-ray radiographs of half-atmosphere xenon shocks with iron walls. (a) Pure xenon fill (b) xenon plus 3% propane. The graph shows the ultra violet radiation mean free path for the latter mixture.

Figure 6: Iridium rail experiments: (a) and (b) are clean metal rails. In (c) the left hand rail was coated with machinist's oil. (d) is a cross-section of the magnetic shear experiment, showing (1) the xenon fill (2) the plastic insulator plated with $\approx$ 50 mm of aluminum (3) the iridium-plated rails, and (4) the iron pole pieces of a strong electromagnet. (e) and (f) are experiments with the sheared magnetic field.

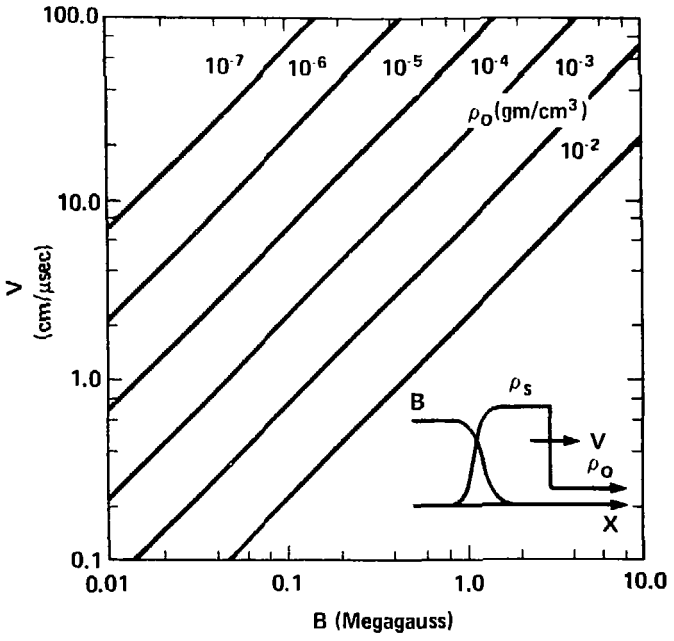
100.0
10.0
1.0
0.1
0.01
0.1
1.0
10.0
V
(cm/μsec)
B (Megagauss)
10^{-7}
10^{-6}
10^{-5}
10^{-4}
10^{-3}
10^{-2}
ρ_o(gm/cm^3)
B
ρ_s
V
ρ_o
X

Fig. 1

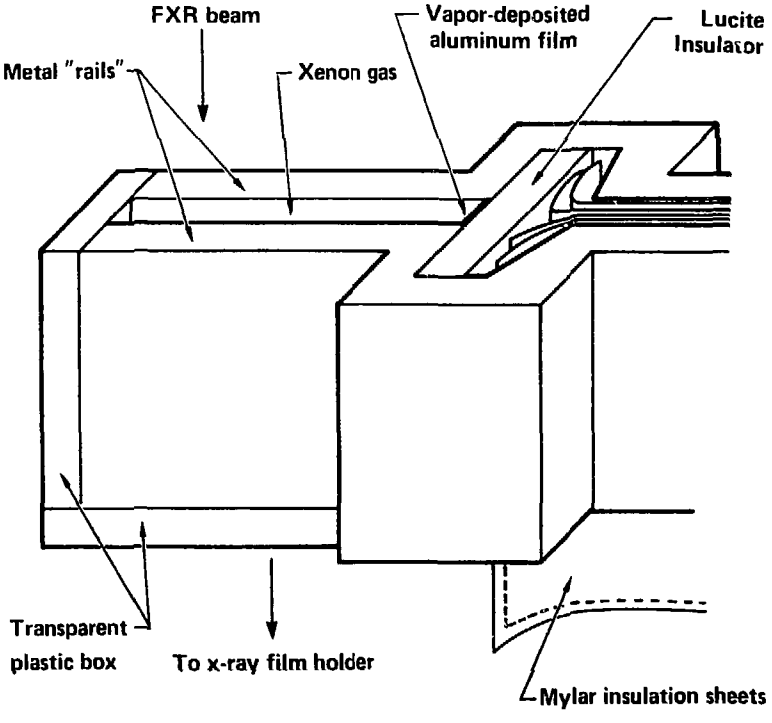
FXR beam
Vapor-deposited aluminum film
Lucite Insulator
Metal "rails"
Xenon gas
Transparent plastic box
To x-ray film holder
Mylar insulation sheets

Fig. 2

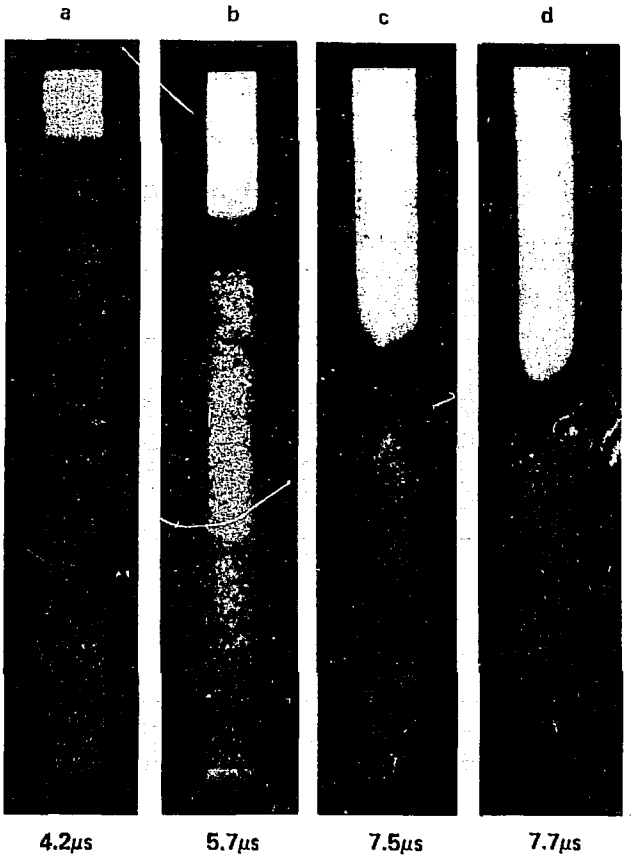

Fig. 3

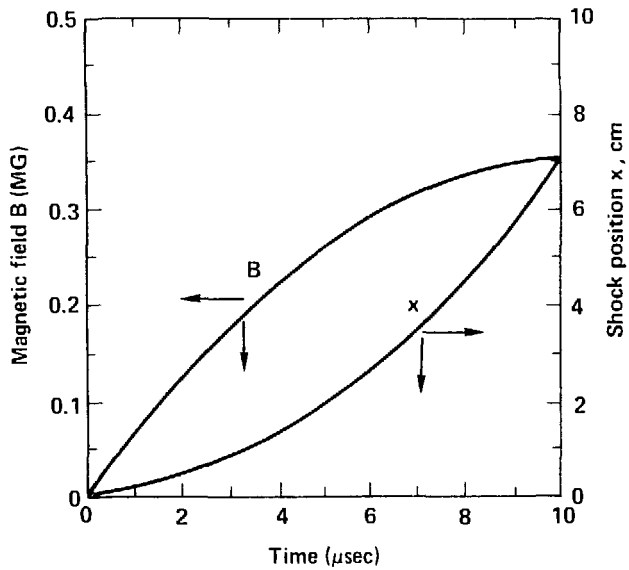
0.5
0.4
0.3
0.2
0.1
0
Magnetic field B (MG)
10
8
6
4
2
0
Shock position x , cm
B
x
0
2
4
6
8
10
Time (μsec)

Fig. 4

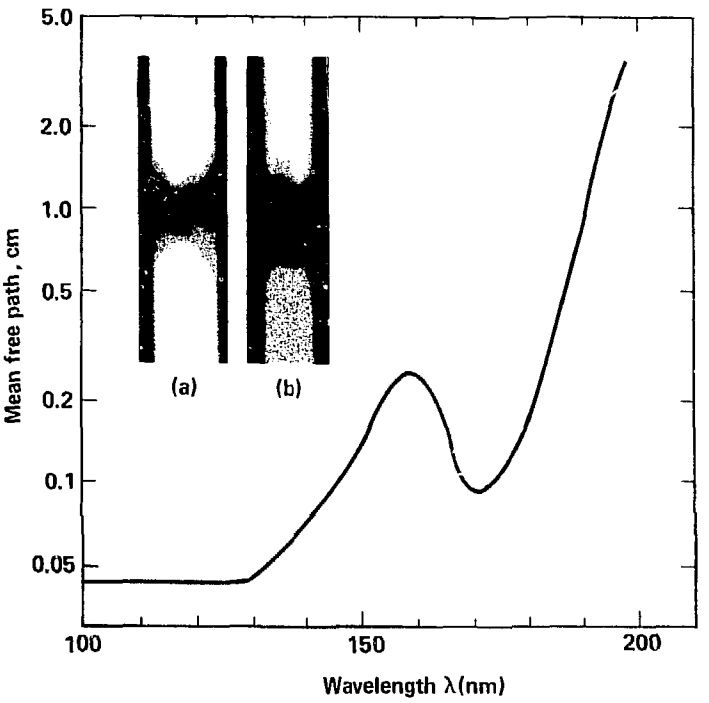
5.0
2.0
1.0
0.5
0.2
0.1
0.05
Mean free path, cm
(a)
(b)
100
150
200
Wavelength λ(nm)

Fig. 5

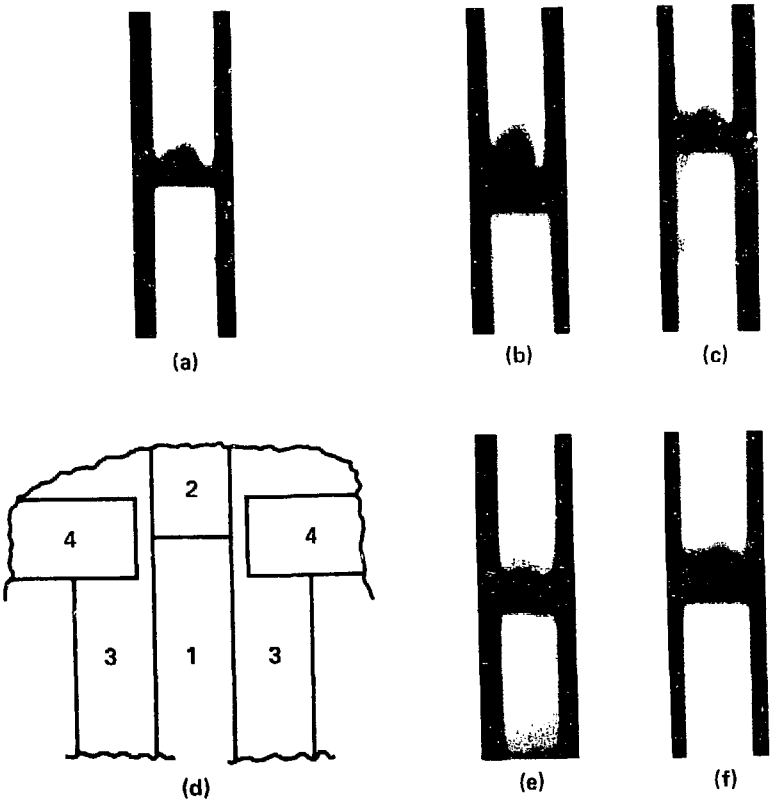

Fig. 6